Charting the molecular network of the drug target Bcr-Abl

Marc Brehme[a,1], Oliver Hantschel[a,1], Jacques Colinge[a], Ines Kaupe[a], Melanie Planyavsky[a], Thomas Köcher[b], Karl Mechtler[b], Keiryn L. Bennett[a], and Giulio Superti-Furga[a,2]

[a]Research Center for Molecular Medicine, Austrian Academy of Sciences, Lazarettgasse 19, 1090 Vienna, Austria; and [b]Research Institute of Molecular Pathology, Dr. Bohrgasse 7, 1030 Vienna, Austria

Edited by John Kuriyan, University of California, Berkeley, CA, and approved March 13, 2009 (received for review January 22, 2009)

The tyrosine kinase Bcr-Abl causes chronic myeloid leukemia and is the cognate target of tyrosine kinase inhibitors like imatinib. We have charted the protein–protein interaction network of Bcr-Abl by a 2-pronged approach. Using a monoclonal antibody we have first purified endogenous Bcr-Abl protein complexes from the CML K562 cell line and characterized the set of most tightly-associated interactors by MS. Nine interactors were subsequently subjected to tandem affinity purifications/MS analysis to obtain a molecular interaction network of some hundred cellular proteins. The resulting network revealed a high degree of interconnection of 7 ''core'' components around Bcr-Abl (Grb2, Shc1, Crk-I, c-Cbl, p85, Sts-1, and SHIP-2), and their links to different signaling pathways. Quantitative proteomics analysis showed that tyrosine kinase inhibitors lead to a disruption of this network. Certain components still appear to interact with Bcr-Abl in a phosphotyrosine-independent manner. We propose that Bcr-Abl and other drug targets, rather than being considered as single polypeptides, can be considered as complex protein assemblies that remodel upon drug action.

chronic myeloid leukemia | imatinib | protein interaction network | tyrosine kinase inhibitor

Drug targets are typically regarded as single proteins or even protein fragments. This traditional view is based on the fact that high-throughput screening of large compound libraries, still the most commonly used approach to identify lead compounds in drug discovery, mainly assays binding or inhibition of proteins or protein fragments (1, 2). In line with this approach, the action of drugs in a cellular context is commonly envisaged as the interaction of the drug with a single or very limited number of cellular proteins. In strong contrast to this reductionist view, modern postgenomic technologies, in particular large-scale interaction proteomics and drug/chemical proteomics approaches, have dramatically changed our view of the organization of the human proteome and drug action. Proteins very rarely act in isolation, but are organized as part of large multiprotein complexes/molecular machines that may dynamically change their spatial and temporal organization (3–5). Along this line, unbiased proteomics approaches for drug targets have shown that most drugs that were considered highly specific often interact with a larger number of previously-unidentified target proteins that themselves are even part of larger protein complexes (6, 7). In line with these insights, pharmacogenomic studies suggest that dozens, if not hundreds, of gene products affect the efficacy of drugs in individuals (8). Furthermore, drugs often have undesired side effects by impinging on different pathways that, in turn, may be shared by different diseases (9, 10). These insights have changed our view of drug action. Instead of considering the alteration of the activity of a single protein by a drug, the action of a drug may have pleiotropic effects on a number of different proteins, leading to a perturbation of molecular networks at different levels (including changes in gene expression, post-translational modifications, protein–protein interactions, and metabolites).

The Bcr-Abl tyrosine kinase and its small-molecule inhibitors, such as imatinib, served as a paradigmatic case for modern targeted cancer therapy. Bcr-Abl is formed by a reciprocal chromosomal translocation event [t9;22 (q34;q11)] that leads to the fusion of the breakpoint cluster region (BCR) gene and the Abelson tyrosine kinase (ABL1), thereby generating a deregulated, constitutively-activated tyrosine kinase (11). Expression of Bcr-Abl is considered to be sufficient for the transformation of hematopoietic stem cells leading to chronic myeloid leukemia (CML) in humans and a CML-like myeloproliferative disorder in mice (12, 13). The central role of Bcr-Abl in the pathophysiology of CML led to the development of the highly-specific Bcr-Abl inhibitor imatinib (Gleevec) that is now the frontline therapy for CML in all disease stages (14). The occurrence of secondary imatinib resistance leading to patient relapse and disease progression led to the development and approval of the second-generation inhibitors nilotinib and dasatinib that target most imatinib-resistant Bcr-Abl variants (15). However, the general shortcomings of primary and secondary resistance, especially in advanced disease stages, and long-term tolerability of Bcr-Abl inhibitors remain a major clinical problem (16). Considering the inability of current Bcr-Abl inhibitors to target leukemia stem cells, we aim to study the molecular repertoire and the cellular circuitry that Bcr-Abl does participate in, which may be a useful way to identify possible additional targets in the Bcr-Abl signaling network that may be exploited for combination therapy (17).

Bcr-Abl expression leads to the phosphorylation and activation of a large number of key signaling components (18). Furthermore, Bcr-Abl, which itself is phosphorylated on numerous tyrosine residues, leads to the recruitment of a set of proteins containing Src homology 2 (SH2) and/or phosphotyrosine binding (PTB) domains, and Bcr-Abl binds to tyrosine-phosphorylated proteins via its own SH2 domain. Thereby, Bcr-Abl is thought to be assembled in a multiprotein complex (19–22).

Aware of the existing extensive, but heterogeneous data on Bcr-Abl interacting proteins, substrates, and downstream signaling components, we undertook a systematic and unbiased approach to study the Bcr-Abl protein interaction network with the aim to complement the existing data and provide a more consolidated view on Bcr-Abl protein interaction partners. We decided to use a defined cellular setting and concentrate on the immediate interactors of Bcr-Abl. We purified endogenous Bcr-Abl protein complexes from CML cells and identified its associated proteins by MS and focused on 18 proteins that appeared to interact with Bcr-Abl at high stochiometry. Using tandem affinity purifications of 9 of these Bcr-Abl interactors,

Author contributions: M.B., O.H., J.C., and G.S.-F. designed research; M.B., O.H., and I.K. performed research; J.C., M.P., T.K., K.M., and K.L.B. contributed new reagents/analytic tools; M.B., O.H., J.C., M.P., T.K., K.M., K.L.B., and G.S.-F. analyzed data; and O.H. and G.S.-F. wrote the paper.

The authors declare no conflict of interest.

This article is a PNAS Direct Submission.

Freely available online through the PNAS open access option.

[1]M.B. and O.H. contributed equally to this work.

[2]To whom correspondence should be addressed. E-mail: gsuperti@cemm.oeaw.ac.at.

This article contains supporting information online at www.pnas.org/cgi/content/full/0900653106/DCSupplemental.

www.pnas.org/cgi/doi/10.1073/pnas.0900653106

statistical analysis of the protein interaction network identified a set of 7 proteins that was most highly interconnected with Bcr-Abl, compatible with the notion of a Bcr-Abl "core" complex. Importantly, we show that inhibition of Bcr-Abl kinase activity by tyrosine kinase inhibitors resulted in the complete disruption of some interactions, whereas others were partly retained or remodeled in the presence of the drugs.

Results

Proteomic Identification of the Endogenous Bcr-Abl Multiprotein Complex. To identify endogenous interactors of Bcr-Abl, we immunoprecipitated Bcr-Abl/c-Abl protein complexes from cell lysates of the CML cell line K562 by using the monoclonal Abl antibody 24-21 (23) (Fig. 1*A*). Mapping the epitope of this antibody showed that it recognizes the αII-αIII loop in the C-terminal F-actin binding domain present in both Bcr-Abl and c-Abl (residues 1094–1096), which is not involved in F-actin binding or any other known protein–protein interaction (24) (Fig. 1*B*). Bcr-Abl/c-Abl and interacting proteins were isolated by using covalently-coupled Abl antibody and eluted with detergent. Elution fractions that contained most Bcr-Abl were pooled, separated by 1D SDS/PAGE and analyzed by MS. Searching the MS data against the human IPI protein database yielded a primary dataset of 427 proteins (25) (Table S1). In parallel, we identified the 708 proteins most prevalent in the total cell lysate of K562 cells representing the K562 core proteome (26) (Table S2). Based on this list of proteins, specific proteins were identified by comparing pull-down versus core proteome datasets by applying the SAM statistical test (27). This statistical procedure, gauged at 5% false discovery rate, yielded 18 high confidence interactors of Bcr-Abl/c-Abl with a sequence coverage that would be compatible with a high stoichiometry interaction (Table S3). As expected, a number of these 18 Bcr-Abl/c-Abl complex component candidates were known interactors of Bcr-Abl and are well-described signaling proteins (Table S3). Grb2, Shc1, and Crk-I are adapter proteins containing SH3, SH2, and PTB domains that serve as adapter interfaces in tyrosine kinase signaling (28). p85α and β are 2 of 5 regulatory subunits that associate with the catalytic subunit of phosphatidylinositol-3-kinase (29). The E3-ubiquitin ligases c-Cbl and Cbl-B typically bind and ubiquitinate activated tyrosine kinases and negatively regulate their activity (30). SHIP-2 is a SH2 domain-containing phosphatidylinositol-5-phosphatase known to bind the Abl SH3 domain and, via its PTB domain, Shc with yet unknown function in Bcr-Abl signaling (31). Sts-1 (suppressor of T cell receptor signaling 1) was initially identified as a JAK2 interactor containing an SH3 domain. Subsequently, Sts-1 was described as a negative regulator of the EGF receptor, ZAP70, and Syk, which can be attributed to the presence a noncanonical tyrosine phosphatase domain in the C terminus of the protein (32, 33). Sts-1 is a hitherto undescribed interactor of Bcr-Abl and may be a novel regulator or antagonist of Bcr-Abl action. The remaining interactors belong to the clathrin-mediated endocytic machinery, including different adapter protein 2 (AP2) complex subunits (AP2α1, AP2β1, AP2μ1), the epidermal growth factor receptor substrate 15 (Eps15), Stonin-2 (STN2), BMP-2-inducible protein kinase (BMP2K/BIKE), and RALBP1-associated EPS domain-containing protein (REPS1) (34) (Table S3). In addition to the 18 interactors compatible with stoichiometric interactions, we identified many previously-characterized Bcr-Abl/c-Abl interacting proteins, such as Abi-1, Abi-2, DNA-PK, WAVE-2, SHP-2, and Crk-L, but with lower peptide counts (35) (Table S1).

As the Abl immunoprecipitation experiment of endogenous complexes did not allow us to distinguish between interactors of Bcr-Abl and c-Abl, we engineered K562 cell lines expressing versions of c-Abl (autoinhibited) the constitutively-active c-Abl PP (36) variant fused to a tandem affinity purification (TAP) tag (37). In both cases, purifications from K562 cells yielded large amounts of the c-Abl bait protein, but none of the 18 interactors described above (Table S4). Thus, these are bona fide Bcr-Abl interactors.

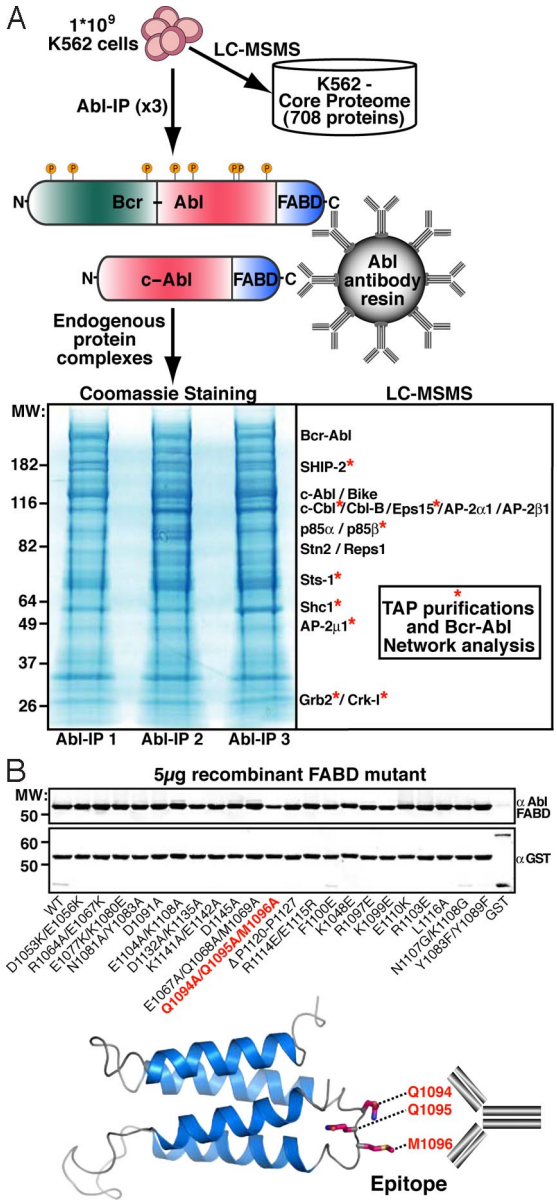

Fig. 1. Proteomic identification of endogenous Bcr-Abl interactors. (*A*) Immunoprecipitation of endogenous Bcr-Abl/c-Abl protein complexes was performed in 3 technical repeats, and eluates were stained with Coomassie. Bcr-Abl/c-Abl interactors marked with a red asterisk were used as bait for TAP purifications. (*B*) The epitope of the Abl 24-21 antibody was mapped by using mutants of the Abl F-actin binding domain and is shown on the structure of the Abl F-actin binding domain (Protein Data Bank ID code 1ZZP) 24. Only mutation of residues Q1094, Q1095, and M1096 showed reduced binding of the antibody.

Bcr-Abl Protein Network Analysis. We performed TAP complex purifications of Bcr-Abl interacting proteins from K562 cells with a 2-fold aim: (*i*) to obtain reciprocal confirmatory data on the interaction with Bcr-Abl of the individual proteins and (*ii*) to perform a topological analysis of the enlarged network obtained from the entire analysis. Of the 18 putative Bcr-Abl complex members, we chose Shc1, SHIP-2, Crk-I, Grb2, Sts-1, and 1 member each of the Cbl and p85 families (c-Cbl and p85β, respectively). Of all of the proteins thought to be involved in the AP2 adapter complex, we chose to analyze 2 representative members (Eps15 and AP2μ1), taking amenability and size into account. All 9 TAP purifications were performed as biological duplicates and statistically significant interactors were identified by using core proteome

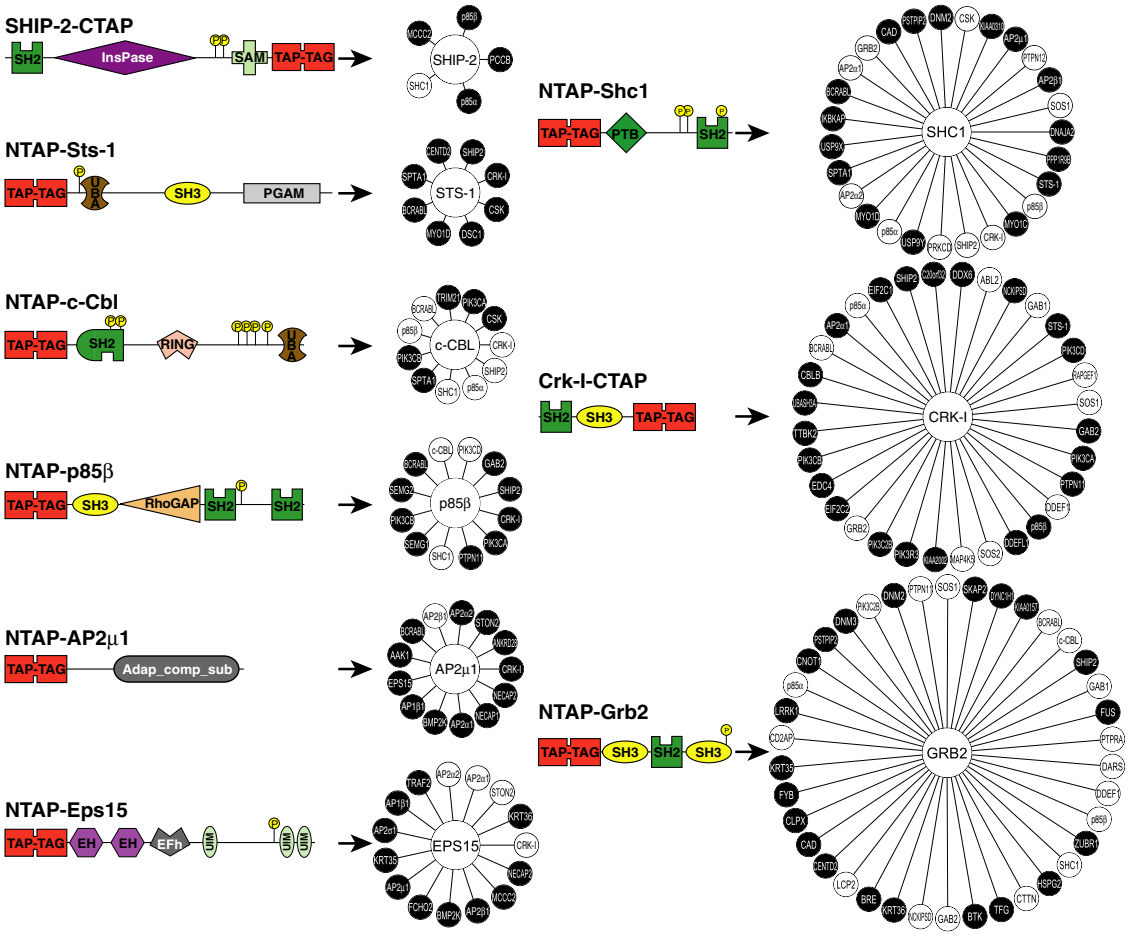

Fig. 2. TAP purifications with 9 Bcr-Abl interactors. Schematic representation of the domains and known tyrosine phosphorylation sites of the 9 Bcr-Abl interactors that were tagged on their N or C terminus and subjected to TAP. Identified interactors are represented as star diagrams with the respective bait protein in the middle. Interactors that had been annotated in HPRD or IntAct are shown as white circles, and black circles represent potential novel interactions. A list of all proteins identified in the TAP purifications is in Table S4.

enrichment (Fig. 2 and Table S5). In all cases the bait protein was identified abundantly in the final TAP eluate by immunoblotting and MS analysis (Table S5 and Fig. S1). Each of the 9 bait proteins identified a number of known interactors, validating the experimental approach, whereas ≈2/3 of all interactors may be considered as novel according to the Human Protein Reference Database (HPRD) or IntAct database (Fig. 2). This dataset enriches the still scanty database of human MS-analyzed protein–protein interactions. Not unexpectedly, the small SH2/SH3/PTB domain containing adapter proteins Grb2, Shc1, and Crk-I displayed most interactors, many of which link to important downstream signaling pathways (Fig. 2). Rewardingly, all bait proteins, with the exception of Eps15 and AP2μ1, interacted with at least half of the other bait proteins, including Bcr-Abl.

The combination of the datasets from the 9 TAP purifications resulted in a single coherent protein–protein interaction network around the 9 bait proteins embedding Bcr-Abl in its center. Analysis of the network topology revealed a high level of interconnectivity (Fig. 3). To monitor the significance and degree of interconnectivity, we considered k-cores in the network (38). A k-core is a subnetwork containing at least k nodes, where each node is linked to at least k other nodes. For example, in a 4-core (i.e., $k = 4$) each node is connected to at least 4 other members of the protein network constituting the 4-core network. Generation of randomized networks shows that the 4-core (consisting of Bcr-Abl, SHIP-2, c-Cbl, p85α/β, Sts-1, Shc1, Grb2, and Crk-I as nodes) is significant at the 10^{-5} level. Interestingly, if Sts-1 is excluded, the closer Bcr-Abl interactors form an even more connected 5-core (Fig. 3, red halo). The 2 TAP baits of the AP2 adaptor complex (Eps15 and AP2μ1) display 3 (AP2μ1) and only 1 edge (Eps15) to the members of the 5-core and are therefore positioned more distantly in the network (Fig. 3, blue halo).

To limit the possible bias introduced by the a priori selection of the 9 bait proteins, where a protein that was not initially selected as Bcr-Abl interactor could have a reduced connectivity with the complex around Bcr-Abl, we represent the TAP-MS results as an undirected graph, meaning that the edges between the nodes in the network do not contain directionality information on the interactions. Therefore, a link created from a bait protein is also valid starting from its prey. To assess the significance of our finding of a 4- and 5-core, we performed network randomization simulations. Generating 10^5 different randomized networks resulted only in 2- and 3-cores in approximately equal proportion (Fig. 3*B*, gray histogram), but no k-cores with $k > 3$. Therefore, the observed 4- and 5-core networks are statistically highly significant ($P < 10^{-5}$; Fig. 3*B*, red and blue line graph).

In conclusion, the unbiased network analysis of the TAP dataset showed that Eps15 and AP2μ1 form an 11-member 2-core complex (AP2α1, AP2α2, AP2β1, AP2μ1, AP1β1, BIKE, Eps15, NECAP2, stonin-2) that included Shc1 and Crk-I (Fig. 3, blue halo). This finding raised the possibility that AP2 adapter complex-mediated intracellular trafficking is functionally linked to the Bcr-Abl com-

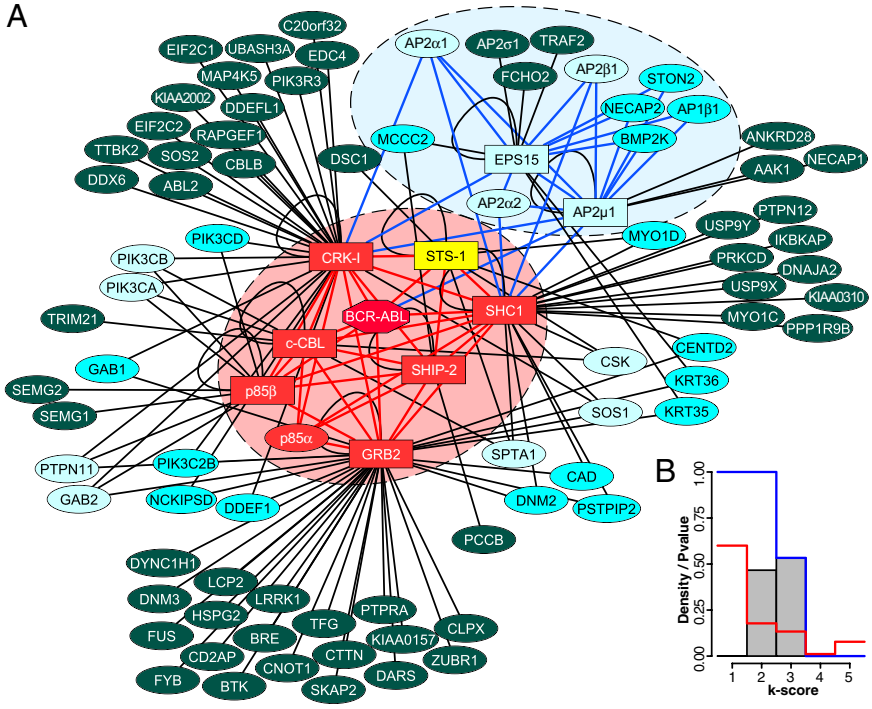

Fig. 3. The Bcr-Abl protein network. (*A*) Combination of the 9 TAP purification datasets results in a single protein–protein interaction network. The 9 TAP bait proteins are shown as rectangles, Bcr-Abl is diamond shape, and all other identified interactors are ellipses. The 4-core Bcr-Abl core complex is highlighted in red, and the associated AP2 adapter complex is highlighted in blue. Interactors with 3, 2, or 1 edges to the Bcr-Abl core network are shown in light blue, turquoise, and dark green, respectively. The figure was created by using Cytoscape. (*B*) Randomized network simulations yield only 2 or 3 cores. The gray histogram shows the proportion (density) of random networks that contain a *k*-core with the highest possible *k*. The blue line graph shows the *P* value of a *k*-core deduced from the histogram. The red line graph represents the proportion (density) of proteins in the network that are found in a *k*-core with highest possible *k* for $k = 1, 2, 3, 4, 5$. Therefore, the experimentally-observed 4-core and 5-core networks are statistically highly significant.

plex in analogy to the function of the AP2 adapter complex in receptor tyrosine kinase trafficking. Clearly, Bcr-Abl is most intimately interconnected with SHIP-2, c-Cbl, p85α/β, Shc1, Sts-1, Grb2, and Crk-I, which we define as the 8-member Bcr-Abl core complex (4). From all that is known about the biology of p85α and p85β, it is unlikely that both p85 isoforms may have a different binding mode or be present simultaneously in the Bcr-Abl core complex. Therefore, for the remainder of the article, both isoforms will be treated equally.

The network analysis also revealed some proteins interacting with 3 different Bcr-Abl core interactors, each (Fig. 3*A* and Fig. S2*A*; light blue nodes). These included spectrin-α, 2 of the catalytic subunits of phosphatidylinositol-3-kinase (p110α and p110β), the SH2-domain containing tyrosine phosphatase SHP-2, the tyrosine kinase Csk, the Grb2 adapter binding protein Gab2, and the guanine nucleotide exchange factor Sos1. Many of these proteins are protooncogenes and have been described to form critical links to downstream signaling pathways (p110α/β for the PI3K/Akt pathway; Sos1, Gab2, and SHP-2 for the Ras/MAPK pathway) and were shown to be necessary for Bcr-Abl dependent transformation, e.g., SHP-2 and Gab2 (39, 40).

Impact of Tyrosine Kinase Inhibitors on the Bcr-Abl Core Complex. The tyrosine kinase inhibitors nilotinib and dasatinib are very potent inhibitors of Bcr-Abl and successfully used to treat CML patients (15). Dasatinib targets the active conformation of Bcr-Abl and has a markedly broader specificity compared with the highly selective nilotinib, which targets a unique inactive Bcr-Abl conformation, as does imatinib (7, 41). To monitor the impact of these tyrosine kinase inhibitors on the integrity and composition of the Bcr-Abl complex, we treated K562 cells with dasatinib and nilotinib for 3 h at concentrations ≈10 times higher than their respective IC_{50} values for Bcr-Abl. Under these conditions, Bcr-Abl kinase activity and Bcr-Abl-dependent signal transduction is effectively suppressed (48). We immunoprecipitated Bcr-Abl complexes from drug- and mock-treated cells and analyzed the samples by immunoblotting against the Bcr-Abl interactors (Fig. 4*A*). In addition, we performed relative quantification by MS using iTRAQ labeling (42) (Fig. 4 *B* and *D*). Whereas Bcr-Abl immunoprecipitated with equal efficiency from mock-, dasatinib-, and nilotinib-treated K562 cells, a strong decrease in the interaction of all 7 core interactors was observed in the presence of the drugs. Interaction of Bcr-Abl with c-Cbl, Sts-1, Shc1, and Crk-I was undetectable upon drug treatment,

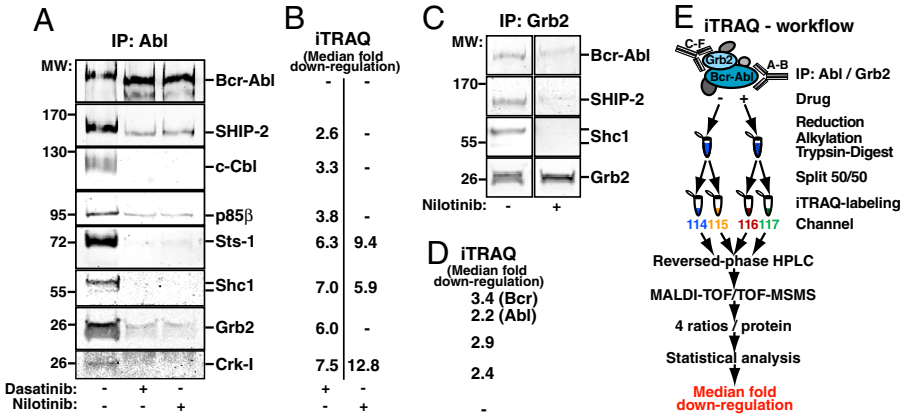

Fig. 4. Nilotinib and dasatinib remodel the Bcr-Abl complex. (*A*) Bcr-Abl protein complexes were immunoprecipitated from mock-, dasatinib-, and nilotinib-treated K562 cells and immunoblotted against Bcr-Abl and the 7 core interactors. (*B*) Quantitative MS analysis using iTRAQ labeling comparing dasatinib-treated versus mock-treated and nilotinib-treated versus mock-treated Bcr-Abl immunoprecipitates. (*C*) Grb2 protein complexes were immunoprecipitated from mock- and nilotinib-treated K562 cells and immunoblotted against Grb2, Bcr-Abl, SHIP-2, and Shc1. (*D*) Quantitative MS analysis using iTRAQ labeling comparing nilotinib- versus mock-treated Grb2 immunoprecipitates. (*E*) Workflow outlining the iTRAQ labeling strategy used for this study. Eluates were reduced, alkylated, digested with trypsin, split in half, and labeled with 2 different isobaric tags each.

BIOCHEMISTRY

whereas the residual binding of SHIP-2, p85β, and Grb2 to Bcr-Abl could be detected in the presence of both drugs (Fig. 4*A*). In line with these results, interaction of all 7 core members with Bcr-Abl was found to be reduced by dasatinib by using relative quantification by MS. In another iTRAQ experiment we compared mock- and nilotinib-treated samples. Here, Crk-I, Sts-1, and Shc1 showed reduced binding to Bcr-Abl (Fig. 4*B*). Interestingly, Crk-I, Sts-1, and Shc1, which were undetectable in Abl immunoprecpitates from drug-treated cells, also showed the strongest reduction in binding to Bcr-Abl (>5-fold) in both quantitative MS experiments (Fig. 4 *A* and *B*). Notably, SHIP-2 showed the mildest reduction (2.5-fold) in binding to Bcr-Abl by dasatinib in the MS experiment and residual interaction with Bcr-Abl could be detected by immunoblotting. To analyze changes in protein complex composition of a specific Bcr-Abl interactor, we immunoprecipitated Grb2, probed for Bcr-Abl and the selected core interactors, and performed relative quantification by using iTRAQ in the presence and absence of nilotinib. Reduced binding of Bcr-Abl, SHIP-2, and Shc1 to Grb2 was detected by iTRAQ and immunoblotting (Fig. 4 *C* and *D*).

Altogether, these experiments show that the Bcr-Abl complex is severely affected by the drug treatment, but at the same time that individual interactions are affected differentially, so that one can still detect a postdrug protein complex. These experiments prompts us to conclude that Bcr-Abl tyrosine kinase inhibitors are targeting the Bcr-Abl complex, leading to its remodeling rather than "just" binding to the Bcr-Abl kinase domain.

Discussion

We have performed 2 independent, but connected, lines of experiments that led to the characterization of what we would like to propose as the Bcr-Abl core complex in CML cells. We started out to identify the native endogenous Bcr-Abl complex, which led to a list of 18 candidate interactors for which the semiquantitative parameter of sequence coverage by MS was compatible with the association being stoichiometric in nature. The protein interaction network of 9 of the candidates (excluding Bcr-Abl as bait) was therefore determined by using TAP to enable a statistical analysis of the resulting protein network topology. The network showed that 8 proteins (including Bcr-Abl) were significantly more connected with each other than with any other of the hundred proteins in the analysis or compared with control random networks. Other proteins of the 18 candidate interactors formed different subnetworks presumably more loosely connected to Bcr-Abl and likely to represent modules exerting cellular household functions (such as the AP2 adapter complex). We believe that the 2 approaches offer convincing evidence for the existence of an 8-component Bcr-Abl containing multiprotein complex of high stoichiometry. Such a complex, taking Bcr-Abl tetramerization into account, is calculated to exceed 2.5 MDa. All of our attempts to obtain confirmation of the size of the intact complex by sucrose density gradients, gelfiltration, or native gel electrophoresis combined with chemical cross-linking were frustrated by the failure to yield homogenous results. This result is likely to reflect the general difficulty to measure protein assemblies in solution that are close to the size limits of the technologies and the relatively low affinity and dynamics by which the mainly SH2/SH3 domain-dependent interactions of this particular complex appears to depend on. In addition, alternative complexes with different (mutually-exclusive) constituents may exist that in principle cannot be identified with the TAP-MS approach and ensuing network analysis. Finally, future studies will have to confirm the set of Bcr-Abl interactors in cell lines other than K562.

TAP and other 2-step affinity purification strategies have proven to be a robust technology for the characterization of protein complexes and are known to reliably identify rather sturdy interactions of either high-affinity and/or favorable kinetic parameters (e.g., low k_{off} rates) (43). Therefore, many interactions that had been described in the literature, some that are critical for Bcr-Abl function, may have evaded detection by TAP because they may be less sturdy, less stoichiometric, or confined to other particular cells or conditions. A large group of Bcr-Abl interactors are likely to include Bcr-Abl substrate proteins that are just phosphorylated by Bcr-Abl without engaging in an interaction intimate enough to survive 2 affinity purification steps. In this study, we have focused on the core components of Bcr-Abl interacting proteins that form a platform that link the Bcr-Abl core complex to different signal transduction pathways and is embedded in a wider signal transduction network, including major downstream transcriptional targets, such as STAT5 or Myc (22).

The TAP-MS approach with the 9 selected baits resulted in the identification of a large number of novel interactors. In addition, through unbiased protein identification by MS, the approach confirmed several previously-identified interactors of most bait proteins, in particular, of the intensively-studied SH2-containing adapter proteins. This dataset significantly increases the existing protein–protein interactions of the bait proteins and will be a valuable resource for the scientific community.

The prominent identification of the 5-inositol phosphatase SHIP-2 and the protein tyrosine phosphatase Sts-1 as a novel Bcr-Abl interactor is interesting to note as both proteins have been described as negative regulators in different signal transduction pathways (32, 44). Sts-1 was shown to strongly dephosphorylate different tyrosine kinases. Elucidating the molecular and functional details of the Sts-1 Bcr-Abl interaction should be the object of future studies.

The Bcr-Abl core complex is a complex assembly of 8 different proteins with many different domains and a complex interaction mode. Most notably, it carries 3 different enzymatic activities caused by the presence of the tyrosine kinase domain in Bcr-Abl, a tyrosine phosphatase domain in Sts-1, and a 5-inositolphosphatase domain in SHIP-2. Future studies will need to address whether all enzymatic domains are activated in the Bcr-Abl core complex and whether alternative pharmacological targeting may be of benefit in combination with tyrosine kinase inhibitor treatment to overcome drug resistance or disease relapse.

One of the most interesting findings of our study is the ability of tyrosine kinase inhibitors to remodel the Bcr-Abl core complex. Upon inhibition of Bcr-Abl kinase activity with dasatinib or nilotinib, a severe reduction in the interactions of 4 of 7 core interactors with Bcr-Abl was detected, likely to be caused by the inhibition of Bcr-Abl tyrosine kinase activity and the ensuing global loss of tyrosine phosphorylation in K562 cells. As a consequence, SH2- and PTB domain-mediated interactions were abolished, whereas interactions that are independent of tyrosine phosphorylation could be maintained. Furthermore, because tyrosine phosphorylation may also allosterically change domain conformations or intramolecular interactions, protein–protein interactions may remodel in the presence of tyrosine kinase inhibitors. Indeed, we observed that certain interactions were only reduced, but not abolished in the presence of drug. Therefore, we propose a "post drug complex" that may be assembled differently, because residually bound Bcr-Abl interactors may have switched their molecular interaction mode. Thus, rather than simple "loss of function," the molecular mode of action of nilotinib and dasatinib can be described as system perturbations that leads to a dynamic remodeling of the protein–protein interaction space. This finding may represent a paradigm for the characterization of drug targets in the postgenomic era, but it needs further experimental support beyond the Bcr-Abl core complex.

Materials and Methods

DNA Constructs. cDNAs were obtained from RZPD (Crk-I, Grb2, Sts-1, Eps15, AP2μ1) or OriGene Technologies (Shc1, p85β), or they were kindly provided by S. J. Decker (University of Michigan, Ann Arbor, MI) (SHIP-2) and B. J. Mayer (Massachusetts College of Pharmacy and Health Science, Worchester, MA) (c-Cbl). The cDNAs were cloned into the respective destination vectors for

expression as N- or C-terminal fusions to the TAP cassette by using the Gateway cloning system (Invitrogen) (37).

Antibodies. Antibodies used included: Abl (mouse monoclonal, Ab-3; Calbiochem), Abl (rabbit polyclonal, K-12; Santa Cruz), SHIP-2 (rabbit polyclonal; kind gift of D. Wisniewski, Sloan-Kettering Institute, New York), c-Cbl (rabbit polyclonal, produced in-house against recombinant c-Cbl UBA domain), Grb2 (rabbit polyclonal, C-23; Santa Cruz) and Grb2 (mouse monoclonal, clone 81; BD), c-Crk (mouse monoclonal, clone 22; BD), Shc1 (mouse monoclonal, clone 30; BD), Sts-1 (rabbit polyclonal; Rockland), and p85β antiserum (mouse monoclonal, clone T15, AbD; Serotec).

Cell Culture, Immunoprecipitation, and Immunoblot Assays. K562 (DSMZ ACC 10) cells were grown in RPMI medium 1640/10% FCS/1% penicillin/streptomycin. K562 total cell lysates for immunoprecipitation, immunoblot, and TAP experiments were prepared as described (37, 45).

Immunoprecipitation of Endogenous Bcr-Abl Complexes. A total of 1×10^9 K562-cells were lysed in TAP buffer 37, cleared by centrifugation, and incubated with covalently-coupled c-Abl antibodies (Ab-3; Calbiochem 24-21) at 4 °C for 6 h. After washing bound proteins were eluted with 1% SDS.

Generation of Stable Cell Lines and TAP. K562 cells stably-expressing NTAP- or CTAP-fusion entry point proteins were generated by stable transduction by retroviral gene transfer 3. TAPs were performed as described (37).

MS and Bioinformatics. Proteins were separated by SDS/PAGE and visualized by silver or Coomassie staining. Entire gel lanes were sliced into pieces, digested in situ with trypsin (46), purified, concentrated, and analyzed by nano-LC-MSMS (47). Tryptic digests were analyzed by data-dependent nanocapillary reversed-phase LC-MSMS, and proteins were identified by automated database searching. Confident binders were deduced from the TAP samples according to statistical analysis and subsequently linked to each respective Bcr-Abl core complex candidate (see *SI Text* for details).

Tyrosine Kinase Inhibitor Treatment. Dasatinib (Sprycel; BMS-354825) and nilotinib (Tasigna; AMN107) were dissolved in DMSO and used at final concentrations of 100 nM and 1 μM, respectively. K562 cells were mock-, dasatinib-, or nilotinib-treated at the indicated concentrations for 3 h.

Quantitative iTRAQ MS Analysis of Bcr-Abl and Grb2 Complexes in the Presence of Tyrosine Kinase Inhibitors. Bcr-Abl and Grb2 complexes were immunoprecipitated from mock-, dasatinib-, or nilotinib-treated K562 cells. Upon tryptic in-solution digestion each sample was split in half, labeled with iTRAQ reagents (2 channels per sample after splitting), separated with RP-HPLC, and analyzed by MALDI-TOF/TOF tandem MS. Medians of all 4 iTRAQ ratios were determined for each protein followed by statistical analysis of their significance (see *SI Text* for details).

ACKNOWLEDGMENTS. We thank S. Decker for SHIP-2 cDNA; B. Mayer for c-Cbl cDNA; D. Wisniewski for SHIP-2 antibody; A. C. Gavin, F. Grebien, C. Baumann, and T. Bürckstümmer for critical reading of the manuscript; and all members of G.S.-F.'s group for help and discussions. This work was supported by Austrian Science Fund Grant P18737, the Austrian Proteomics Platform, and the Austrian Academy of Sciences.

1. Bleicher KH, Bohm HJ, Muller K, Alanine AI (2003) Hit and lead generation: Beyond high-throughput screening. *Nat Rev Drug Discov* 2:369–378.
2. Brown D, Superti-Furga G (2003) Rediscovering the sweet spot in drug discovery. *Drug Discov Today* 8:1067–1077.
3. Bouwmeester T, et al. (2004) A physical and functional map of the human TNF-α/NF-κB signal transduction pathway. *Nat Cell Biol* 6:97–105.
4. Gavin AC, et al. (2006) Proteome survey reveals modularity of the yeast cell machinery. *Nature* 440:631–636.
5. Kuriyan J, Eisenberg D (2007) The origin of protein interactions and allostery in colocalization. *Nature* 450:983–990.
6. Bantscheff M, et al. (2007) Quantitative chemical proteomics reveals mechanisms of action of clinical ABL kinase inhibitors. *Nat Biotechnol* 25:1035–1044.
7. Rix U, et al. (2007) Chemical proteomic profiles of the BCR-ABL inhibitors imatinib, nilotinib, and dasatinib reveal novel kinase and nonkinase targets. *Blood* 110:4055–4063.
8. Evans WE, McLeod HL (2003) Pharmacogenomics: Drug disposition, drug targets, and side effects. *N Engl J Med* 348:538–549.
9. Yildirim MA, Goh KI, Cusick ME, Barabasi AL, Vidal M (2007) Drug-target network. *Nat Biotechnol* 25:1119–1126.
10. Campillos M, Kuhn M, Gavin AC, Jensen LJ, Bork P (2008) Drug target identification using side-effect similarity. *Science* 321:263–266.
11. Wong S, Witte ON (2004) The BCR-ABL story: Bench to bedside and back. *Annu Rev Immunol* 22:247–306.
12. Daley GQ, Van Etten RA, Baltimore D (1990) Induction of chronic myelogenous leukemia in mice by the P210bcr/abl gene of the Philadelphia chromosome. *Science* 247:824–830.
13. Van Etten RA (2007) Oncogenic signaling: New insights and controversies from chronic myeloid leukemia. *J Exp Med* 204:461–465.
14. Deininger M, Buchdunger E, Druker BJ (2005) The development of imatinib as a therapeutic agent for chronic myeloid leukemia. *Blood* 105:2640–2653.
15. Quintas-Cardama A, Kantarjian H, Cortes J (2007) Flying under the radar: The new wave of BCR-ABL inhibitors. *Nat Rev Drug Discov* 6:834–848.
16. Schiffer CA (2007) BCR-ABL tyrosine kinase inhibitors for chronic myelogenous leukemia. *N Engl J Med* 357:258–265.
17. O'Hare T, Eide CA, Deininger MW (2007) Bcr-Abl kinase domain mutations, drug resistance, and the road to a cure for chronic myeloid leukemia. *Blood* 110:2242–2249.
18. Sattler M, Griffin JD (2003) Molecular mechanisms of transformation by the BCR-ABL oncogene. *Semin Hematol* 40:4–10.
19. Salomon AR, et al. (2003) Profiling of tyrosine phosphorylation pathways in human cells using mass spectrometry. *Proc Natl Acad Sci USA* 100:443–448.
20. Steen H, Fernandez M, Ghaffari S, Pandey A, Mann M (2003) Phosphotyrosine mapping in Bcr/Abl oncoprotein using phosphotyrosine-specific immonium ion scanning. *Mol Cell Proteomics* 2:138–145.
21. Hantschel O, Superti-Furga G (2004) Regulation of the c-Abl and Bcr-Abl tyrosine kinases. *Nat Rev Mol Cell Biol* 5:33–44.
22. Ren R (2005) Mechanisms of BCR-ABL in the pathogenesis of chronic myelogenous leukemia. *Nat Rev Cancer* 5:172–183.
23. Schiff-Maker L, et al. (1986) Monoclonal antibodies specific for v-abl- and c-abl-encoded molecules. *J Virol* 57:1182–1186.
24. Hantschel O, et al. (2005) Structural basis for the cytoskeletal association of Bcr-Abl/c-Abl. *Mol Cell* 19:461–473.
25. Kersey PJ, et al. (2004) The International Protein Index: An integrated database for proteomics experiments. *Proteomics* 4:1985–1988.
26. Schirle M, Heurtier MA, Kuster B (2003) Profiling core proteomes of human cell lines by one-dimensional PAGE and liquid chromatography-tandem mass spectrometry. *Mol Cell Proteomics* 2:1297–1305.
27. Tusher VG, Tibshirani R, Chu G (2001) Significance analysis of microarrays applied to the ionizing radiation response. *Proc Natl Acad Sci USA* 98:5116–5121.
28. Pawson T (2007) Dynamic control of signaling by modular adaptor proteins. *Curr Opin Cell Biol* 19:112–116.
29. Zhao L, Vogt PK (2008) Class I PI3K in oncogenic cellular transformation. *Oncogene* 27:5486–5496.
30. Thien CB, Langdon WY (2001) Cbl: Many adaptations to regulate protein tyrosine kinases. *Nat Rev Mol Cell Biol* 2:294–307.
31. Wisniewski D, et al. (1999) A novel SH2-containing phosphatidylinositol 3,4,5-trisphosphate 5-phosphatase (SHIP-2) is constitutively tyrosine phosphorylated and associated with src homologous and collagen gene (SHC) in chronic myelogenous leukemia progenitor cells. *Blood* 93:2707–2720.
32. Mikhailik A, et al. (2007) A phosphatase activity of Sts-1 contributes to the suppression of TCR signaling. *Mol Cell* 27:486–497.
33. Carpino N, et al. (2002) Identification, cDNA cloning, and targeted deletion of p70, a novel, ubiquitously expressed SH3 domain-containing protein. *Mol Cell Biol* 22:7491–7500.
34. Schade AE, et al. (2008) Dasatinib, a small-molecule protein tyrosine kinase inhibitor, inhibits T cellactivation and proliferation. *Blood* 111:1366–1377.
35. Pendergast AM (2002) The Abl family kinases: Mechanisms of regulation and signaling. *Adv Cancer Res* 85:51–100.
36. Barilá D, Superti-Furga G (1998) An intramolecular SH3-domain interaction regulates c-Abl activity. *Nat Genet* 18:280–282.
37. Burckstummer T, et al. (2006) An efficient tandem affinity purification procedure for interaction proteomics in mammalian cells. *Nat Methods* 3:1013–1019.
38. Tong AH, et al. (2002) A combined experimental and computational strategy to define protein interaction networks for peptide recognition modules. *Science* 295:321–324.
39. Chen J, et al. (2007) SHP-2 phosphatase is required for hematopoietic cell transformation by Bcr-Abl. *Blood* 109:778–785.
40. Sattler M, et al. (2002) Critical role for Gab2 in transformation by BCR/ABL. *Cancer Cell* 1:479–492.
41. Hantschel O, Rix U, Superti-Furga G (2008) Target spectrum of the BCR-ABL inhibitors imatinib, nilotinib, and dasatinib. *Leuk Lymphoma* 49:615–619.
42. Ross PL, et al. (2004) Multiplexed protein quantitation in *Saccharomyces cerevisiae* using amine-reactive isobaric tagging reagents. *Mol Cell Proteomics* 3:1154–1169.
43. Gingras AC, Gstaiger M, Raught B, Aebersold R (2007) Analysis of protein complexes using mass spectrometry. *Nat Rev Mol Cell Biol* 8:645–654.
44. Taylor V, et al. (2000) 5′ phospholipid phosphatase SHIP-2 causes protein kinase B inactivation and cell cycle arrest in glioblastoma cells. *Mol Cell Biol* 20:6860–6871.
45. Hantschel O, et al. (2007) The Btk tyrosine kinase is a major target of the Bcr-Abl inhibitor dasatinib. *Proc Natl Acad Sci USA* 104:13283–13288.
46. Shevchenko A, Wilm M, Vorm O, Mann M (1996) Mass spectrometric sequencing of proteins silver-stained polyacrylamide gels. *Anal Chem* 68:850–858.
47. Rappsilber J, Ishihama Y, Mann M (2003) Stop and go extraction tips for matrix-assisted laser desorption/ionization, nanoelectrospray, and LC/MS sample pretreatment in proteomics. *Anal Chem* 75:663–670.
48. Hantschel O, et al. (2008) The chemokine IL-8 and the surface activation protein CD69 are markers for Bcr-Abl activity in CML. *Molecular Oncology* 2(3):272–281.